https://doi.org/10.1093/nargab/lqab112

ChiTaH: a fast and accurate tool for identifying known human chimeric sequences from high-throughput sequencing data

Rajesh Detroja, Alessandro Gorohovski, Olawumi Giwa, Gideon Baum and Milana Frenkel-Morgenstern*

Cancer Genomics and BioComputing of Complex Diseases Lab, Azrieli Faculty of Medicine, Bar-Ilan University, Safed 1311502, Israel

Received June 23, 2021; Revised October 21, 2021; Editorial Decision November 08, 2021; Accepted November 22, 2021

ABSTRACT

Fusion genes or chimeras typically comprise sequences from two different genes. The chimeric RNAs of such joined sequences often serve as cancer drivers. Identifying such driver fusions in a given cancer or complex disease is important for diagnosis and treatment. The advent of next-generation sequencing technologies, such as DNA-Seq or RNA-Seq, together with the development of suitable computational tools, has made the global identification of chimeras in tumors possible. However, the testing of over 20 computational methods showed these to be limited in terms of chimera prediction sensitivity, specificity, and accurate quantification of junction reads. These shortcomings motivated us to develop the first 'reference-based' approach termed ChiTaH (Chimeric Transcripts from High–throughput sequencing data). ChiTaH uses 43,466 non–redundant known human chimeras as a reference database to map sequencing reads and to accurately identify chimeric reads. We benchmarked ChiTaH and four other methods to identify human chimeras, leveraging both simulated and real sequencing datasets. ChiTaH was found to be the most accurate and fastest method for identifying known human chimeras from simulated and sequencing datasets. Moreover, especially ChiTaH uncovered heterogeneity of the BCR-ABL1 chimera in both bulk and single-cells of the K-562 cell line, which was confirmed experimentally.

INTRODUCTION

Gene-gene fusions (or chimeric RNAs generated at the RNA level) typically comprise sequences from two different genes. Fused genes can be generated by different mechanisms, including chromosomal translocations, transcriptional errors, or by *cis*- or *trans*-splicing (1–5). The chimeric RNAs of such joined sequences often serve as cancer drivers, as exemplified by BCR–ABL1, found in ∼95% of chronic myelogenous leukemia (CML) cases (6), by TMPRSS2–ETS, found in ∼50% of instances of prostate cancer (7), and by DNAJB1–PRKACA, the hallmark and likely driver of fibrolamellar carcinoma (8). Identifying such driver fusions in a given cancer or complex disease is important for diagnosis and treatment. For example, tyrosine–kinase inhibitors are highly effective in treating patients suffering from CML and other cancers harboring kinase fusions (9–12). Despite the importance of chimeric RNAs in various cancers, the current terminology used to describe gene-gene fusions can be inconsistent, possibly due to the field's infancy. Presently, numerous terms have been used to describe chimeric RNAs, such as transcription-mediated fusions, fusion genes, conjoined genes, complex genes, chimeras, spanning genes, hybrid genes, and fusion transcripts. In this article, we define chimeric RNAs and fusion genes as chimeras.

Cytogenetic analysis led to the discovery of BCR–ABL1 as the first chimera in 1973 (13). Since, dozens of chimeras have been identified in hematologic cancers. Over the past decade, the advent of high–throughput, low–cost, and sophisticated next-generation sequencing (NGS) technologies, such as DNA-Seq or RNA-Seq, together with improved computational power, has made global identification of chimeras in solid tumors, including sarcoma, carcinoma, and tumors of the central nervous system, possible (14). Today, over 20 computational tools for identifying chimeras using high–throughput sequencing data are available. The common feature of these *de novo* chimera identification methods is the use of discordant and/or split reads to recognize exon-exon junction sites (15–34). At the same time, the various methods vary in terms of the read alignment tool employed, the version of the human reference genome consulted, the gene annotations used, the criteria

*To whom correspondence should be addressed. Tel: +972 722644901; Email: milana.morgenstern@biu.ac.il selected for filtering candidate chimeras, and likely, false positives. Furthermore, these tools were found to be limited in terms of prediction sensitivity and specificity, accurate quantification of junction reads, installation complexity, execution time and robustness when utilizing DNA-Seq or RNA-Seq and paired-end or single-end sequencing data (35–37).

These shortcomings motivated us to develop a first 'reference-based' approach, termed ChiTaH (Chimeric Transcripts from High–throughput sequencing data), for identifying chimeras from both high–throughput DNA-Seq and RNA-Seq sequencing data. Since the introduction of NGS, thousands of human chimeras have been identified and published at NCBI and in the literature (38). Accordingly, we processed 10 100 714 human EST/mRNA sequences from NCBI GenBank and identified 548 262 human chimeric transcripts and collected them into the latest version of our extended ChiTaRS 5.0 database (39). These chimeric transcripts were then used to assemble a reference database of chimeras presenting non–redundant unique junction sequences that included 43 466 humans chimeric RNAs. ChiTaH uses these 43 466 chimeras as a reference database of known human chimeras to map DNA-Seq or RNA-Seq sequencing reads to accurately identify chimeric reads. We subsequently evaluated the performance of ChiTaH and four best chimera detection methods, namely, EricScript (19), STAR-Fusion (16), JAFFA (15), and FusionCatcher (20). We assessed each method on simulated and real sequencing datasets by evaluating various parameters, such as sensitivity and specificity to detect candidate chimeras, quantification of detected junction reads, total time required, and RAM (random–access memory) consumed to complete the analysis. Moreover, we analyzed single-cell RNA-Seq sequencing data collected from the K-562 cell line to assess the potential of ChiTaH to determine BCR-ABL1 chimera heterogeneity and expression at the single cell level. We experimentally confirmed the heterogeneity of BCR-ABL1 in the K562 cell line. Finally, we analyzed RNA-Seq samples of human cancer cell lines from the CCLE (Cancer Cell Line Encyclopedia) to build a catalog of cancer-specific chimeras. We also analyzed, RNA-Seq samples of normal human tissues from ArrayExpress archive of EBI (European Bioinformatics Institute) to build a catalog of normal tissue-specific chimeras, using ChiTaH.

MATERIALS AND METHODS

Collection of known human chimeras

A total of 10 100 714 EST/mRNA sequences were retrieved from the NCBI GenBank database and aligned to a human reference genome (hg38) using the BLAT program (40). EST/mRNA sequences were considered as human chimeras if their first and second sequence tracts shared a minimum identity of 95% and if these two sequences could not be mapped linearly to the human reference genome. In addition, the total length of the two connected mapped nucleotide sequence tracts had to be more than one-third of the length of the original EST/mRNA sequence. Original EST/mRNA sequences with lengths shorter than 21 bp and longer than 75 000 bp were discarded. A total of 548 262 human chimeras were thus identified and included in the latest version of our extended ChiTaRS 5.0 database (39). Pre-processing of the human chimeras was performed to filter out low–quality sequences. As such, chimeras were filtered out if the identities of the gene1 and gene2 sequences to the human reference genome (hg38) were <96%, or if the chimera presented an 'intron–intron' junction type, containing only non–coding sequences in the parental genes. Isoform chimeras with identical parental genes that were identically orientally were removed, as were chimeras with short–length parental genes of less than 50 bp. Following such screening, a total of 74 223 high-quality human chimeras remained (Figure 1A).

Non-redundant known human chimeras

A total of 74 223 (100%) high–quality chimeras were used to prepare human chimeras with non-redundant unique junction sequences. To calculate the junction region of a chimera, the overlap length between the gene1 and gene2 sequences was calculated as follows:

$$\text{Overlap start} = \text{IF}\,(\text{S2} < \text{E1 then S2 else E1})$$

$$\text{Overlap end} = \text{IF}\,(\text{S2} < \text{E1 then E1 else S2})$$

$$\text{Overlap length} = (\text{Overlap end} - \text{Overlap start}) + 1$$

Chimeras with overlap lengths of more than 40 bp were filtered out (Figure 1B). The remaining chimeras were used for the junction length calculations as follows:

$$\begin{aligned}\text{Junction start} &= \text{IF(overlap start} - 15 >\\ &= \text{S1 then overlap start} - 15\text{ else S1)}\\ \text{Junction end} &= \text{IF(overlap end} + 15 <\\ &= \text{E2 then overlap end} + 15\text{ else E2)}\\ \text{Junction length} &= (\text{Junction end} - \text{Junction start}) + 1\end{aligned}$$

To identify non–redundant unique junction regions, stand-alone BLASTn (41) of 65 761 junction sequences were performed against the NCBI curated databases of human genomic sequences (ref_euk_rep_genomes; taxids:9606) and human transcripts (refseq_rna; taxids:9606), a human reference genome (hg38), and a human reference transcriptome (hg38:cDNA) with 95% minimum identity and 100% query coverage. In total, 15 187 (20.46%) chimeras with identical junction sequences as human sequences were filtered out (Figure 1D). The remaining junction sequences were subjected to analysis using dedupe.sh (https://github.com/BioInfoTools/BBMap) to detect duplicate junction sequences by pairwise alignment. In total, 4280 (5.76%) chimeras with duplicate junction sequences were excluded (Figure 1E). The remaining junction sequences were used to calculate the percentage of A, T and N nucleotides, using the faCount (http://hgdownload.cse.ucsc.edu/admin/exe/linux.x86_64/) tool. Chimeras indicative of the possible presence of a poly-A tail or ambiguous nucleotides containing a high percentage of A, T, and N nucleotides at junction sequences were filtered out (Figure 1F). Thus, 43 466 (58.56%) high-quality, non–redundant human chimeras were obtained.

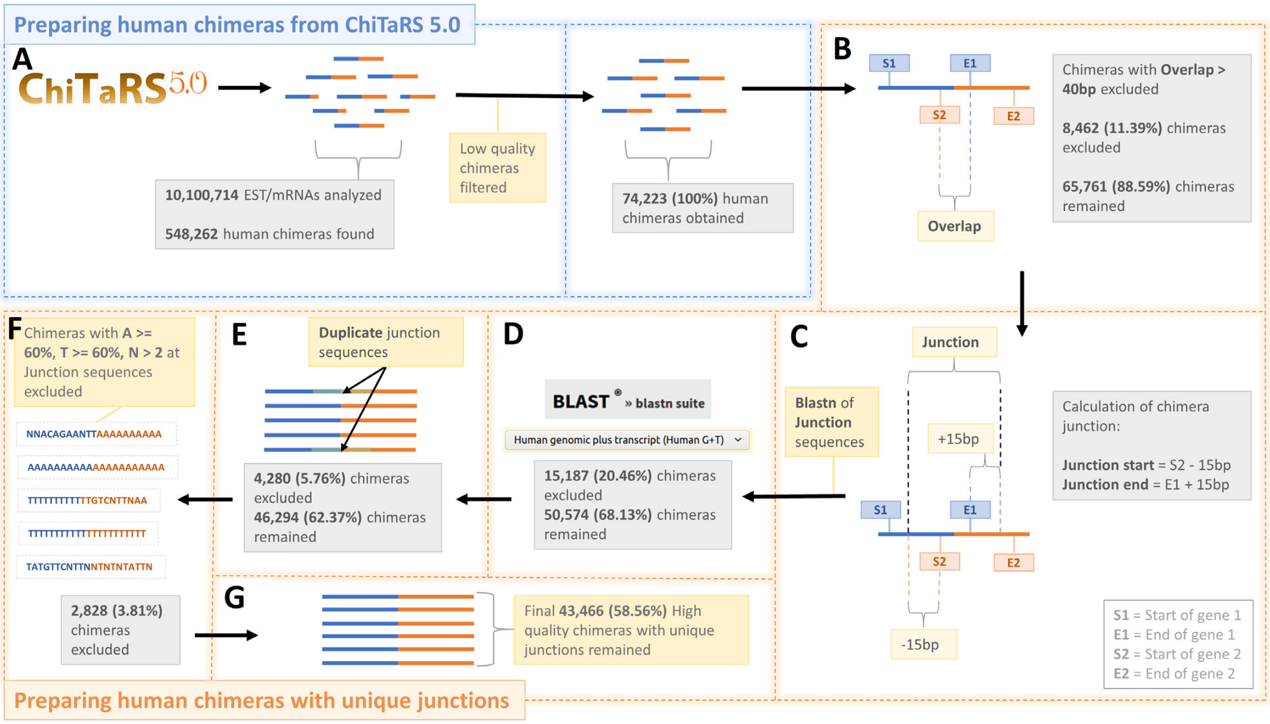
Preparing human chimeras from ChiTaRS 5.0
A
ChiTaRS5.0
10,100,714 EST/mRNAs analyzed
548,262 human chimeras found
Low quality chimeras filtered
74,223 (100%) human chimeras obtained
B
S1
E1
S2
E2
Overlap
Chimeras with Overlap > 40bp excluded
8,462 (11.39%) chimeras excluded
65,761 (88.59%) chimeras remained
C
Junction
Blastn of Junction sequences
+15bp
S1
E1
S2
E2
-15bp
Calculation of chimera junction:
Junction start = S2 - 15bp
Junction end = E1 + 15bp
S1 = Start of gene 1
E1 = End of gene 1
S2 = Start of gene 2
E2 = End of gene 2
D
BLAST® » blastn suite
Human genomic plus transcript (Human G+T)
15,187 (20.46%) chimeras excluded
50,574 (68.13%) chimeras remained
E
Duplicate junction sequences
4,280 (5.76%) chimeras excluded
46,294 (62.37%) chimeras remained
F
Chimeras with A >= 60%, T >= 60%, N > 2 at Junction sequences excluded
NNACAGAANTTAAAAAAAAAA
AAAAAAAAAAAAAAAAAAAA
TTTTTTTTTTTTGTCNTTNAA
TTTTTTTTTTTTTTTTTTTTT
TATGTTCNTTNNTNTNTATTN
2,828 (3.81%) chimeras excluded
G
Final 43,466 (58.56%) High quality chimeras with unique junctions remained
Preparing human chimeras with unique junctions

Figure 1. Collection of non-redundant human chimeras from ChiTaRS 5.0. (**A**) Total number of ESTs/mRNAs analyzed. (**B**) Filtration of chimeras based on overlap length. (**C**) Calculation of chimera junction lengths. (**D**) Filtration of chimeras based on BLAST analysis against human sequences. (**E**) Filtration of chimeras based on duplicate junction sequences by pairwise sequence analysis. (**F**) Filtration of chimeras based on poly-A tail or ambiguous character. (**G**) Final chimeras with non–redundant unique junction sequences.

ChiTaH workflow

ChiTaH uses 43 466 non–redundant unique human chimeras, a human reference genome (hg38), and a human reference transcriptome (hg38:cDNA) as a combined reference to map DNA-Seq or RNA-Seq sequencing reads using the bowtie2 aligner with a local alignment approach (42) (Figure 2B). ChiTaH subsequently calculates chimeric reads mapped at non-redundant unique junction regions of chimeras using bedtools coverage (43). Then, ChiTaH calculates final candidate chimeras and provides the output of all identified chimeras across samples with junction read counts offered in a single matrix table (Figure 2C).

Comparative assessment of chimera detection methods

We sought to comparatively evaluate the performances of ChiTaH and the current best chimera detection methods. Over the past decade, over 20 computational tools for identifying chimeras using high–throughput sequencing data have become available. Earlier studies performed comprehensive evaluation of many of these methods (35–37). Based on their conclusions, we downloaded and installed four tools, i.e., EricScript (19), STAR-Fusion (16), JAFFA (15), and FusionCatcher (20), for benchmarking (Table 1). All four methods and ChiTaH were run on a simulated dataset and bulk RNA-Seq sequencing data at default, using recommended parameters for each method, 25 CPUs, and 1000 Gb of RAM. The sensitivity and specificity of each tool on the simulated dataset were assessed using the following criteria:

1. Sensitivity (%) = (TP/TF) × 100%
2. Positive Predictive Value (PPV) or Specificity (%) = (TP/(TP + FP)) × 100%

TP: True positive, correctly identified known candidate chimeras
TF: Total known chimeras in the simulated dataset
FP: False–positive chimeras identified

For each run of the simulated and bulk RNA-Seq sequencing datasets, the computational RAM used in gigabytes (Gb) and time consumed in minutes to complete the analysis were also calculated.

Simulated dataset

The simulated dataset was generated for comparative assessment analysis of the different chimera detection methods. Sequences of 100 known chimeras in humans were used to assess the sensitivity of each method. The sequence of each of the 100 known chimeras is available at NCBI and contains unique parental genes and non–redundant unique junction sequences. About 95% of known chimeras contain exons in both parental genes, and can thus be translated into protein (Supplementary Figure S1). Human CDS sequences with a minimum of 2000 bp were obtained from Ensemble and merged with sequences of 100 known chimeras to generate an artificial mRNA assembly ∼60 Mb in size, containing a total of 17 163 sequences. This artificial mRNA assembly was used to generate simulated sequencing data using BBMap reformat.sh (https://github.com/BioInfoTools/BBMap). In to-

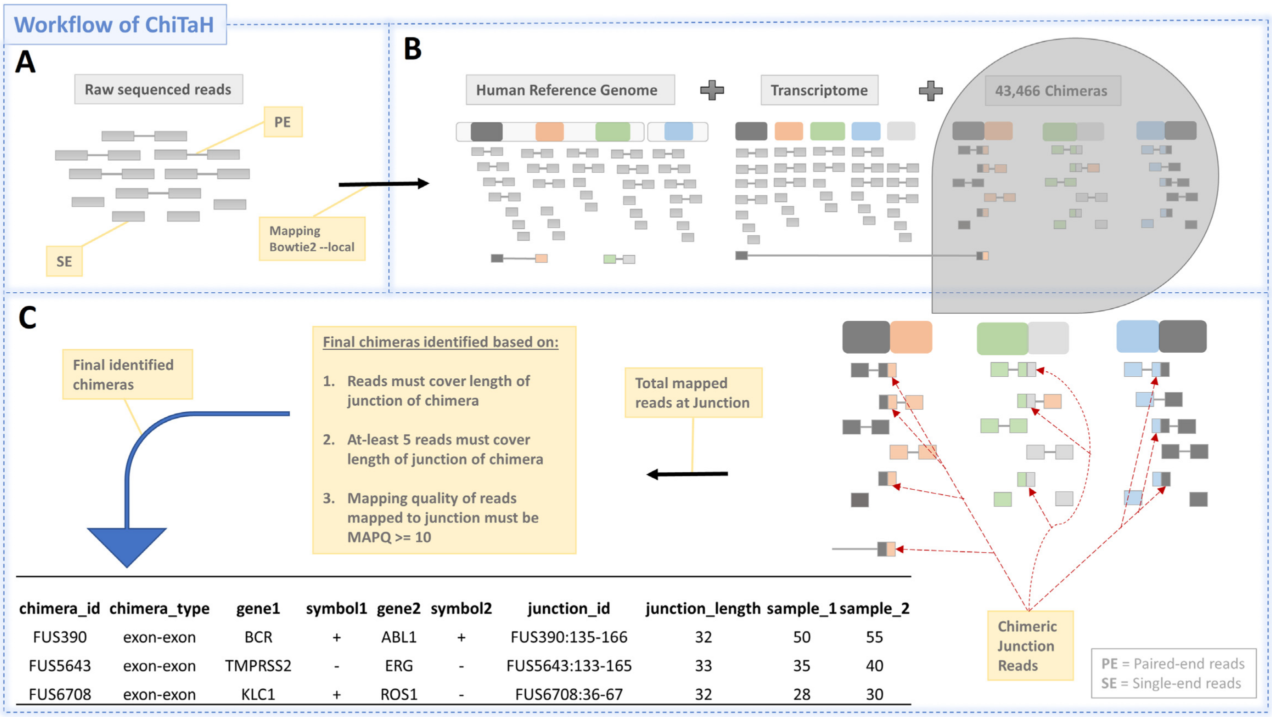

Final chimeras identified based on:

1. Reads must cover length of junction of chimera
2. At-least 5 reads must cover length of junction of chimera
3. Mapping quality of reads mapped to junction must be MAPQ >= 10

chimera_id	chimera_type	gene1	symbol1	gene2	symbol2	junction_id	junction_length	sample_1	sample_2
FUS390	exon-exon	BCR	+	ABL1	+	FUS390:135-166	32	50	55
FUS5643	exon-exon	TMPRSS2	-	ERG	-	FUS5643:133-165	33	35	40
FUS6708	exon-exon	KLC1	+	ROS1	-	FUS6708:36-67	32	28	30

Figure 2. Workflow of ChiTaH. (**A**) Paired-end and single-end NGS sequencing reads as input to ChiTaH. (**B**) Mapping of reads using Bowtie2 against a reference database comprising a human genome, a human transcriptome and 43,466 non–redundant known human chimeras. (**C**) Prediction of candidate chimeras based on calculation of junction reads.

Table 1. Four top-level chimera detection methods used for benchmarking

Tool name	Read type supported	Reference	Version	Sequencing data type	Interface	Alignment algorithm
EricScript	Paired-end	(19)	0.5.5	RNA-Seq	Stand-alone	BWA (44), BLAT (40)
STAR-Fusion	Paired-end & single-end	(16)	1.9.1	RNA-Seq	Stand-alone	STAR (45)
JAFFA	Paired-end & single-end	(15)	2.00	RNA-Seq	Stand-alone	bowtie2 (42), BLAT (40)
FusionCatcher	Paired-end & single-end (150 bp)	(20)	1.20	RNA-Seq	Stand-alone	STAR (45), BLAT (40), bowtie2 (42)

tal, 30, 20, 15 and 10 million paired-end reads of 50, 75, 100 and 150 bp in length were generated, respectively. Additionally, 60, 40, 30 and 20 million single-end reads of 50, 75, 100 and 150 bp in length were also generated, respectively.

Bulk RNA-Seq sequencing dataset

A bulk RNA-Seq sequencing dataset was prepared to evaluate parameters such as total detected junction reads, and time and RAM needed to complete the run of real sequencing data. Three bulk RNA-Seq sequencing samples from the K-562 cell line were downloaded from the NCBI SRA database. This source, positive for the known fusion gene BCR–ABL1, contains about 53, 50 and 54 million paired-end reads of 101 bp for samples SRR9032085, SRR9032086 and SRR9032088, respectively.

Single-cell RNA-Seq sequencing dataset

To assess the potential of ChiTaH to determine the heterogeneity of BCR–ABL1 chimeras and their expression at the single-cell level, single-cell sequences from the K-562 cell line were downloaded from NCBI BioProject accession PRJNA430491. To generate the dataset, the Smart-Seq2 design and BGISEQ-500 platform were used to sequence a total of 81 and 249 single cells as paired-end and single-end reads, respectively.

Dataset of cancer cell lines and normal tissues

To assemble a catalog of cancer-specific fusion genes using ChiTaH, 934 RNA-Seq samples of human cancer cell lines from the CCLE (https://www.ebi.ac.uk/gxa/experiments/E-MTAB-2770/Downloads) and 199 RNA-Seq samples of 32 normal human tissues from the ArrayExpress archive of EBI (https://www.ebi.ac.uk/gxa/experiments/E-MTAB-2836/Downloads) were analyzed.

Hardware, software and statistical analysis

Development and comparative analysis were performed on the RedHat Enterprise Linux 7.4 server of an Intel(R) Xeon(R) CPU E5-2620 v2 server with 25 CPUs and 1000

Gb of RAM. The in-house script for ChiTaH was written in Bash programming. Scripts were applied in the Linux environment. The script of ChiTaH and its dependencies are publicly available at the GitHub directory (https://github.com/Rajesh-Detroja/ChiTaH). Statistical analysis was conducted using in-house scripts written in R programming. Plots were generated using Microsoft Excel and custom in-house scripts written in R programming.

Experimental validation of BCR-ABL1 chimeras in the K562 cell line

Cell culture, RNA isolation, cDNA production, PCR analysis and Sanger sequencing was performed to validate BCR-ABL1 chimeras. K562 cells purchased from ATCC (CCL-243) were cultured in RPMI 1640 with 10% FBS and Penicillin-Streptomycin-Amphotericin B Solution (Biological Industries, Beit Haemek, Israel) at 37°C in 5% CO_2. At 60–80% confluency, cultures were routinely sub-cultured using 0.05% Trypsin-EDTA (Biological Industries). Total RNA was extracted from the cells with a RNeasy Mini Kit (Qiagen, Venlo, Netherlands). RNA quality was assessed with a NanoDrop 1000 spectrophotometer (ThermoFisher, Waltham, MA). cDNA was produced using a High-Capacity cDNA Reverse Transcription Kit (Applied Biosystems; ThermoFisher, Waltham, MA). A forward primer from the BCR gene with the sequence AAGA TGATGAGTCTCCGGGG and a reverse primer from the ABL gene with the sequence GGTCCAGCGAGAAGGT TTTC were used to detect the FUS390 chimera, producing a 172 bp fragment. The same forward primer and a reverse primer with the sequence AATATGGCTTCATCTG CATGGC were used to detect the M19695 chimera, producing a 149 bp fragment. The PCR products were eluted from the gel and subjected to Sanger sequencing by Macrogen Europe, using the same primers.

RESULTS

ChiTaH: a reference-based approach for detection of human chimeras

After pre-processing human EST and mRNA sequences from NCBI, a total of 43 466 high–quality, non–redundant human chimeras were curated. A total of 38 550 (88.69%) chimeras contained 1–10 bp of overlap length, followed by 3652 (8.40%) chimeras containing 11–20 bp overlap length, 855 (1.96%) chimeras containing 21–30 bp overlap length and 409 (0.94%) chimeras containing 31–40 bp overlap length were identified. Each chimera junction length was calculated by adding 15 bp to both sides of the overlap region. Hence, junction length is correlated with overlap length of the chimera. This yielded 38 550 (88.69%) chimeras containing 31–40 bp of junction length, followed by 3652 (8.40%) chimeras containing 41–50 bp of junction length, 855 (1.96%) chimeras containing 51–60 bp of junction length, and 409 (0.94%) chimeras containing 61–70 bp of junction length. Moreover, 25 252 (58%) chimeras contain exons in both parental gene sequences, with the potential of translation into a complete chimeric protein. In contrast, a total of 9004 (21%) and 9210 (21%) chimeras contain intron-exon and exon-intron combinations in their parental gene sequences, respectively, and thus have the potential of translation into a partially chimeric protein (Supplementary Figure S4). ChiTaH uses these chimeras to identify chimeric reads from the DNA-Seq or RNA-Seq sequencing data. Specifically, ChiTaH uses only non–redundant junction regions to identify chimeric reads or chimeras, which makes ChiTaH more accurate and robust when considering paired-end or single-end sequencing reads of variable lengths of more than 35 bp.

Comparative assessment of chimera detection methods using a simulated dataset

ChiTaH and four current best methods, namely, EricScript (19), STAR-Fusion (16), JAFFA (15) and FusionCatcher (20), were run on simulated datasets. For each method, default pre-defined alignment and analysis parameters were used. Using simulated datasets, the performance of each method was evaluated in terms of various parameters, such as sensitivity, specificity, quantification of junction reads, and total time and RAM utilized to complete the analysis. Sensitivity in identifying the 100 known chimeras was first assessed. Sensitivity was calculated by considering the number of known chimeras identified by each method from the total of 100 known chimeras in the simulated datasets (Supplementary Figure S2C, D). The average sensitivity of ChiTaH was found to be 100% for identifying know chimeras from paired-end datasets, followed by FusionCatcher and EricScript, with average sensitivities of 89.75% and 80.75%, respectively. In identifying known chimeras from single-end datasets, the average sensitivity of ChiTaH was found to be 100%, followed by FusionCatcher and JAFFA, with average sensitivities of 89% and 81.50%, respectively (S4 File).

Specificity or positive predictive value (PPV) was next assessed to identify known chimeras. Specificity (%) was calculated by considering both the number of known chimeras and the number of false-positive chimeras identified by each method from simulated datasets (Supplementary Figure S2E, F). The average specificity of ChiTaH in identifying chimeras from paired-end datasets was found to be 100%, followed by STAR-Fusion and FusionCatcher, with average specificities of 92.40% and 88.02%, respectively. In identifying chimeras from single-end datasets, the average specificity of ChiTaH was found to be 100%, followed by STAR-Fusion and FusionCatcher, with average specificities of 92.34% and 84.76%, respectively.

The ability to accurately estimate the expression or abundance of identified known chimeras by counting junction reads was next determined. To calculate identified junction reads by each method, a total of 45 commonly identified known chimeras by all five methods in paired-end and/or single-end simulated datasets were listed. Next, a total number of average simulated junctions reads generated for these 45 chimeras was calculated. Thus, on average, 25.91 and 27.88 simulated junctions read were generated for 45 chimeras in paired-end and single-end datasets, respectively. These were considered as control (Min-Expected). From paired-end datasets, ChiTaH identified an average of 28.41 junction reads, followed by STAR-Fusion and EricScript, which identified an average of 25.76 and 22.66 junction reads, respectively. In single-end datasets, ChiTaH identified an average of 29.92 junction reads, followed by STAR-Fusion and FusionCatcher, which identified an average of 24.54 and 23.27 junction reads, respectively (Figure 3E, F). Moreover, it was noted that ChiTaH identified a few more junction reads than expected, possibly because the sensitivity of ChiTaH also allows for the recognizing of junction reads presenting mutations.

The total time in minutes used by each method to complete runs on the simulated datasets was next determined. START-Fusion utilized an average of 9.5 minutes to complete runs of paired-end datasets followed by ChiTaH and FusionCatcher which utilized an average of 11.32 and 51.96 min, respectively. Where, to complete runs of single-end datasets ChiTaH utilized an average of 2.96 min followed by STAR-Fusion and JAFFA which utilized an average of 7.99 and 224.24 min respectively (Figure 4A, B). Finally, the total RAM consumed in Gb by each method to complete analysis of the run-on simulated datasets was assessed. ChiTaH consumed an average of 4.52 Gb of RAM to complete runs of paired-end datasets followed by EricScript and JAFFA which consumed an average of 18.87 and 20.82 Gb of RAM. To complete runs of single-end datasets, ChiTaH utilized an average of 4.32 Gb of RAM, followed by JAFFA and FusionCatcher, which consumed 9.53 Gb and 34.19 Gb of RAM, respectively (Figure 4C, D). Altogether, comparative benchmarking of ChiTaH and the four other methods on simulated datasets found ChiTaH to be the most accurate and fastest method for identifying known human chimeras, followed by STAR-Fusion.

Comparative assessment of chimera detection methods using real sequencing datasets

After benchmarking all five methods on simulated datasets, correlation of the same results with real sequencing datasets was tested. For this, three bulk RNA-Seq samples from the myelogenous leukemia K-562 cell line, namely, SRR9032085, SRR9032086 and SRR9032088, were downloaded from SRA. In these sequencing datasets, the true number of chimeras was not known. As such, parameters such as sensitivity and specificity could not be assessed. Nevertheless, the K-562 cell line-derived samples are positive for the chimera BCR-ABL1, allowing for evaluation of the quantification of BCR-ABL1 junction reads, the total time required, and RAM utilized. Each method was run on the K-562 cell line sequencing datasets using the same server, 25 CPUs, and 1000 Gb of RAM. The total number of junctions reads detected by each method was first calculated. ChiTaH detected an average of 119.33 BCR-ABL1 junctions reads, followed by STAR-Fusion and EricScript, which detected an average of 99.33 and 83 junctions reads, respectively (Figure 5A).

The total time in minutes used to complete the run by each method was also determined. STAR-Fusion utilized an average of 19.97 minutes, followed by ChiTaH and JAFFA, which utilized an average of 33.86 and 171.72 min, respectively. Finally, the total RAM in Gb to complete the run by each method was assessed. ChiTaH consumed an average of 4.67 Gb of RAM, followed by JAFFA and EricScript, which consumed an average of 16.36 and 23.49 Gb of RAM, respectively (Figure 4E, F). Thus, again in agreement with the results obtained using the simulated datasets, ChiTaH and STAR-Fusion were found to be the most accurate and fastest method to identify BCR-ABL1 chimeras from real sequencing datasets of K-562 cell line.

Expression of BCR-ABl1 chimeras in bulk and single cells of the K-562 cell line

BCR-ABL1 chimera was detected by all five methods from bulk RNA-Seq of the K-562 cell line. However, ChiTaH uniquely identified two different chimeric sequences of BCR-ABL1, namely FUS390 and M19695. FUS390 contains exons in both of the parental genes, with the potential of being translating into a complete chimeric protein, while M19695 contains exons in the BCR gene and introns in the ABL1 gene, with the potential of being partially translated into a chimeric protein. A total of 76, 103 and 96 FUS390 junction reads were identified from samples SRR9032085, SRR9032086 and SRR9032088, respectively. A total of 38, 25 and 20 M19695 junction reads were identified from samples SRR9032085, SRR9032086 and SRR9032088, respectively (Figure 5C). To confirm differences at the sequence level, more than 100 bp of junction sequences of FUS390 and M19695 were aligned using the EBI ClustalW (46) program. The alignment of junction sequences showed BCR gene regions to be identical between FUS390 and M19695, while ABL1 regions were unrelated. Further, in order to validate two different version of BCR-ABL1 chimeras in the K562 cell line, we performed a PCR assay designed to detect and amplify these chimeras in K-562 cell cDNA. The PCR product were of the expected sizes. The product was eluted from the gel and subjected to Sanger sequencing with the same primers used for PCR amplification. The sequencing results of both DNA strands were identical to the sequences found by ChiTaH, confirming the presence of FUS390 and M19395 chimeras in the K-562 cell line (Supplementary Figure S5).

Taken together, this result shows the existence of two different versions of BCR-ABL1 chimeras in the K-562 cell line, namely, FUS390, with significantly high expression, and M19695, with significantly low expression (*P*-value: 0.042) (Figure 5B). Based on the discovery of distinct BCR-ABL1 chimeras by ChiTaH in bulk RNA-Seq data of K-562 cells, it was hypothesized that these differences in the BCR-ABL1 chimera could be due to cellular heterogeneity in the K-562 cell line at the single-cell level. To validate this hypothesis, a publicly available total of 81 and 249 K-562 cell line single cells with RNA-Seq sequencing data as paired-end and single-end reads, respectively, were downloaded and analyzed using ChiTaH. With the paired-end single-cell dataset, BCR-ABL1 chimeras were found in a total of 12 (14.81%) cells, with the FUS390 chimera being found in 9 (11.11%) cells, and the M19695 chimera being found in 3 (3.70%) cells. In the single-end single-cell dataset, BCR-ABL1 chimeras were found in a total of 16 (6.41%) cells, with the FUS390 chimera being found in 11 (4.41%) cells, and the M19695 chimera being found in 5 (2%) of cells. In the paired-end or single-end datasets, no cells containing both versions of the BCR-ABL1 chimera were detected. Furthermore, the expression of each chimera in the cell was normalized to RPM (reads per million) and

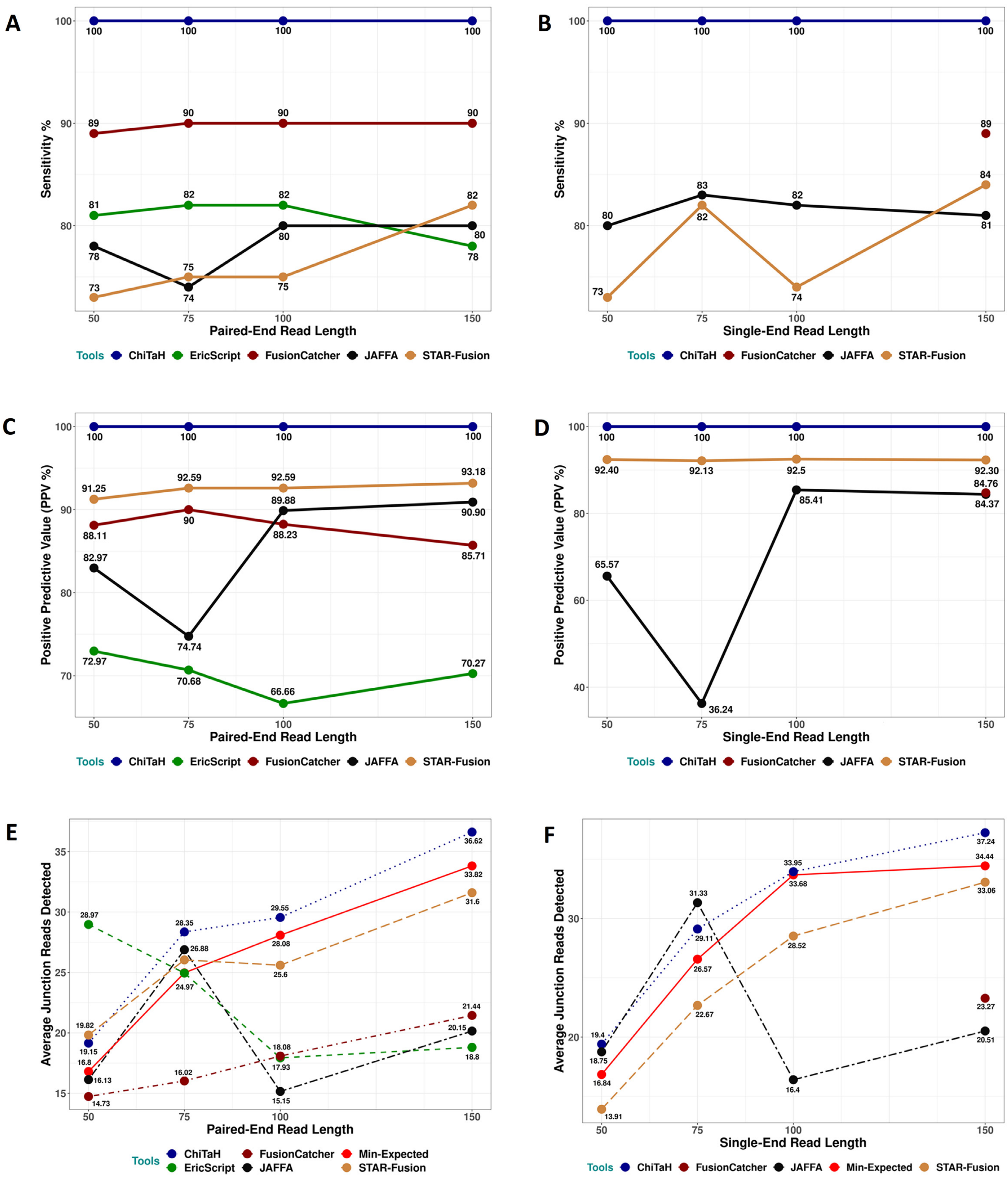

Figure 3. Comparative assessment of ChiTaH using simulated datasets. (**A**) Sensitivity (%) of the five methods tested on paired-end simulated datasets. (**B**) Sensitivity (%) of four methods on single-end simulated datasets. (**C**) PPV (%) of the five methods on paired-end simulated datasets. (**D**) PPV (%) of four methods on single-end simulated datasets. (**E**) Average junction reads detected by the five methods from paired-end simulated datasets. (**F**) Average junction reads detected by four methods from single-end simulated datasets.

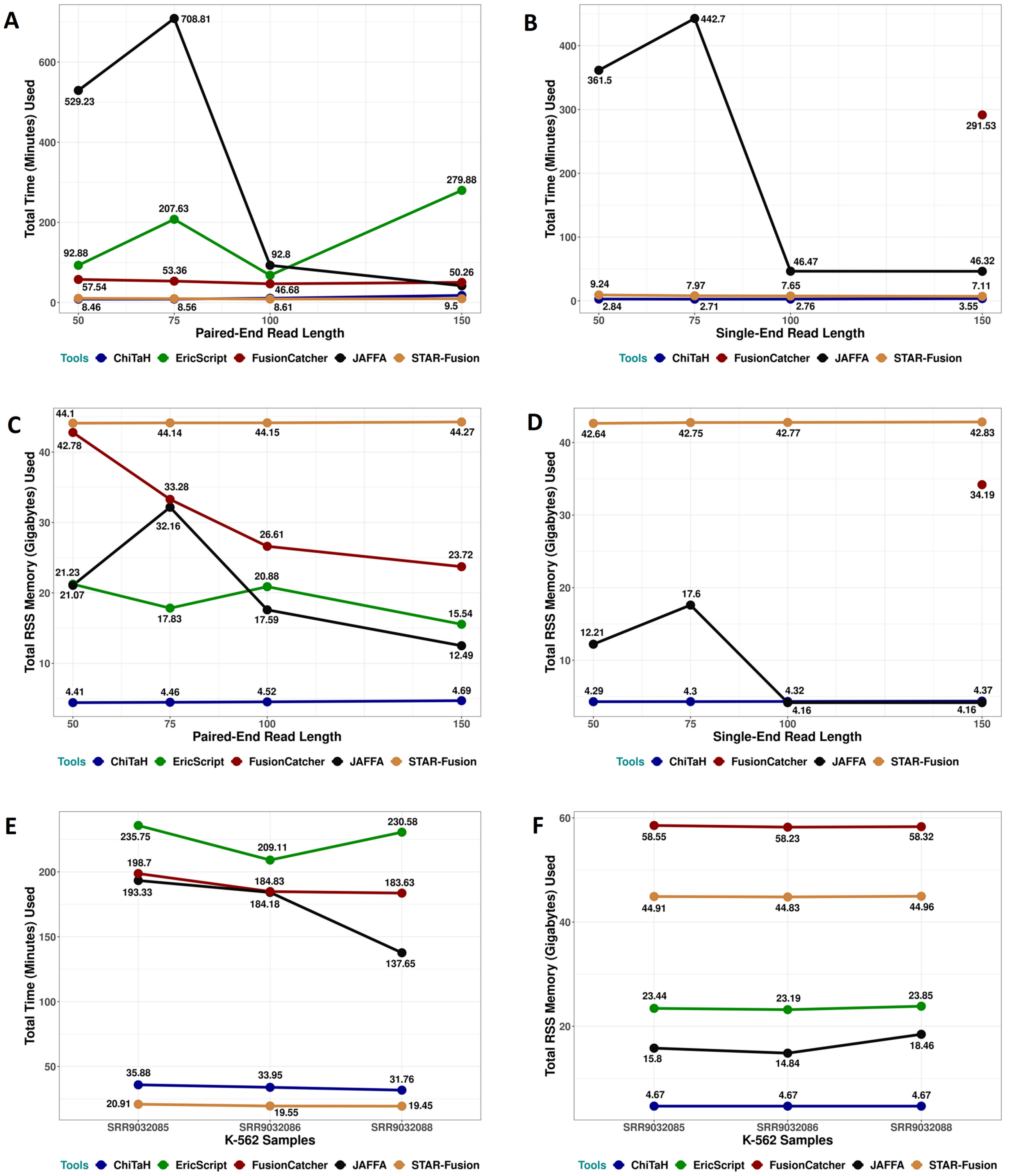

Figure 4. Comparative assessment of ChiTaH using simulated and real datasets. (**A**) Total time in minutes used by the five methods to complete a run of paired-end simulated datasets. (**B**) Total time in minutes used by four methods to complete a run of single-end simulated datasets. (**C**) Total memory in Gb used by the five methods to complete a run of paired-end simulated dataset. (**D**) Total memory in Gb used by four methods to complete a run of single-end simulated datasets. (**E**) Total time in minutes used by the five methods to complete a run of the K-562 cell line sequencing datasets. (**F**) Total memory in Gb used by the five methods to complete a run of the K-562 cell line sequencing datasets.

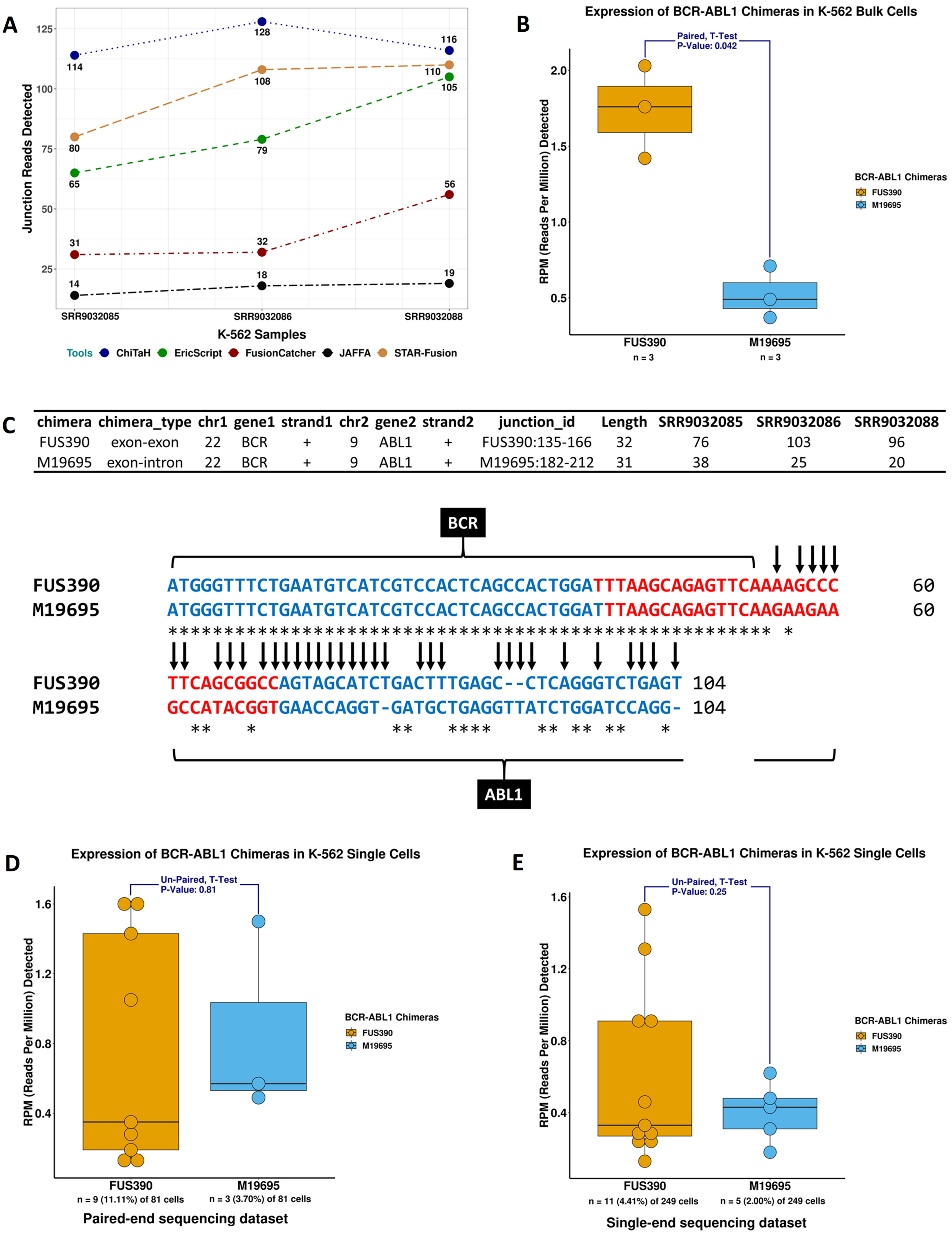

chimera	chimera_type	chr1	gene1	strand1	chr2	gene2	strand2	junction_id	Length	SRR9032085	SRR9032086	SRR9032088
FUS390	exon-exon	22	BCR	+	9	ABL1	+	FUS390:135-166	32	76	103	96
M19695	exon-intron	22	BCR	+	9	ABL1	+	M19695:182-212	31	38	25	20

```
FUS390    ATGGGTTTCTGAATGTCATCGTCCACTCAGCCACTGGATTTAAGCAGAGTTCAAAAGCCC    60
M19695    ATGGGTTTCTGAATGTCATCGTCCACTCAGCCACTGGATTTAAGCAGAGTTCAAGAAGAA    60
          ****************************************************** *

FUS390    TTCAGCGGCCAGTAGCATCTGACTTTGAGC--CTCAGGGTCTGAGT 104
M19695    GCCATACGGTGAACCAGGT-GATGCTGAGGTTATCTGGATCCAGG- 104
            **   *            **   ****    ** ** **   *
```

Figure 5. Expression of BCR-ABL1 chimeras calculated by ChiTaH. (**A**) Total junction reads detected by the five methods in the K-562 cell line sequencing datasets. (**B**) Expression of BCR-ABL1 chimeras in the K-562 cell line bulk RNA-Seq dataset. (**C**) ChiTaH identified a distinct junction in BCR-ABL1 in the K-562 cell line bulk RNA-Seq dataset. (**D**) Expression of BCR-ABL1 chimeras in the K-562 cell line paired-end single-cell dataset. (**E**) Expression of BCR-ABL1 chimeras in the K-562 cell line single-end single-cell dataset.

an unpaired t-test was performed to compare the expression of FUS390 and M19695 at the single cell level. With paired-end or single-end single-cell data, no significant differences were found between the expression of FUS390 and M19695 (Figure 5D, E), which is completely distinct from what was observed with the bulk RNA-Seq data. This discrepancy could be due to the significantly lower expression of FUS390 in most of the cells. Overall, these finding support the presented hypothesis and revealed the heterogeneity of BCR-ABL1 chimeras at the single-cell level using ChiTaH. Unlike other chimera detection methods, ChiTaH identified chimeras at the bulk and single-cell levels and was quite accurate in detecting heterogeneity in known human chimeras.

Chimera analysis of cancer cell lines and normal human tissues

To build a catalog of cancer-specific chimeras using ChiTaH, 934 RNA-Seq samples of human cancer cell lines from the CCLE and 199 RNA-Seq samples of 32 normal human tissues from the ArrayExpress archive of EBI were analyzed. In the CCLE, 934 cell lines of 26 different cancer tissues were sequenced, including 173, 162, 54, 50 and 49 cancer samples from lung, hematopoietic/lymphoid tissues, large intestine, breast, and central nervous system, respectively (Supplementary Figure S3A). After analysis of these datasets using ChiTaH, a total of 2066 and 7673 chimeras were found in the EBI and CCLE samples, respectively. Of these, 1717 chimeras were found to be common to the EBI and CCLE lists, and were considered as normal population chimeras (S2 File) (S3 File). A total of 5956 chimeras were found to be unique to the CCLE cancer samples, and were considered as cancer-specific chimeras (S1 File). Distribution of the junction type in the 5956 chimeras showed that about 3666 (62%) chimeras contain exons in both parental genes, with the potential of being translated into a complete chimeric protein, while 1133 (19%) and 1157 (19%) chimeras contained exon-intron and intron-exon pairs in their parental genes, with the potential to be partially translated into a chimeric protein (Supplementary Figure S3B, C). A total of 3073, 3060, 2009, 1946 and 1568 chimeras were identified from the cancerous lung, hematopoietic/lymphoid tissues, large intestine, breast, and central nervous system, respectively. Moreover, a total of six distinct versions of the BCR-ABL1 chimera was found across 14 cell lines of hematopoietic and lymphoid tissues in the CCLE samples. In agreement with the results for the bulk and single cell RNA-Seq datasets, chimera FUS390 was found to be highly expressed and chimera M19695 was determined to be lowly expressed in the K-562 cell line from the CCLE. The BCR-ABL1 chimera KT696168 was found in a total of eight cell lines of hematopoietic and lymphoid tissues. Chimeras FUS391 and FUS390 were seen in five cell lines, M19695 was noted in two cell lines, and FUS2195 and MH401088 were detected in only a single cell line.

We considered 2066 chimeras found in normal tissues of EBI as population reference chimeras. This population chimeras can be used to filter out chimeras that are frequently expressed in normal human tissues and do not associate with complex diseases, such as cancer. Next, 5956 cancer-specific chimeras found in CCLE cancer cell lines were used for downstream biological analysis. First, a list of unique fusion genes for each cancer was prepared to classify them as a driver gene, oncogene, or tumor suppressor gene. This list was uploaded to the CancerMine (47) database for annotation. Such annotation provides biological insight in terms of fusion genes and their classification as driver, onco-, or tumor suppressor genes for each cancer (S5 File). Moreover, 1647 unique fusion genes from all cancers were uploaded into WebGestalt (48) for gene ontology analysis. The enrichment of these genes shows their significant association with pathways in cancers, such as the Ras signaling pathway, focal adhesion, and proteoglycans in cancer (FDR ≤ 0.05) (Supplementary Figure S6).

DISCUSSION

Access to an accurate and rapid chimera detection method is important both in cancer and complex disease research and for the precision medicine pipeline. With the advent of NGS technologies, global identification of chimeras became feasible. However, despite the development of over 20 computational methods designed to identify chimeras from high-throughput sequencing data, prediction sensitivity, specificity, accurate quantification of junction reads, execution time and hardware requirements remain challenging. Therefore, we developed ChiTaH, a fast 'reference-based' approach for the discovery of known human chimeras with superior accuracy. Currently, ChiTaH contains total of 43 466 non-redundant unique human chimeras combining exons of their parental genes, and thus with the potential of being translated into chimeric proteins.

In all scenarios tested, ChiTaH out-performed the current best methods for identifying chimeras. Specifically, in simulated datasets, ChiTaH out-performed these other methods in terms of sensitivity, specificity, estimating junction reads, execution time, and RAM required to complete the analysis (Figures 3 and 4). The same conclusion was drawn in the case of a true sequencing dataset from the K-562 cell line. The sole limitation in testing ChiTaH is that this tool cannot identify chimeras that are not available in its reference database of known human chimeras. Despite this limitation, the pipeline presented here is entirely customizable, such that user can easily incorporate known chimeras in which they are interested. Moreover, we have been updating our database ChiTaRS on a daily basis since 2012, resulting in addition of thousands of new known human chimeras annually (39, 49–51).

Finally, a unique future of ChiTaH reported here is the ability to identify variable junctions of the same chimera. Of all five tested methods, only ChiTaH discovered two distinct BCR-ABL1 chimeras in the K-562 cell line bulk RNA-Seq dataset, as well as in the single-cell RNA-Seq data. ChiTaH also accurately determined that BCR-ABl1 chimera FUS390 was significantly highly expressed, while chimera M19695 was poorly expressed in the bulk RNA-Seq dataset from K-562 cells. However, in the case of the single cell RNA-Seq dataset from K-562 cells, no significant differences between the expression of FUS390 and M19695 were noted, likely because chimera FUS390 was found to be expressed at only low levels in the majority of K-

562 cells (Figure 5). Moreover, hundreds of RNA-Seq samples from EBI and CCLE were analyzed in just one month, showing that ChiTaH is well suited to meet the demands of large-scale tumor or population sample screening. In summary, the unique features of ChiTaH that allow it to utilize non–redundant junction sequence data for the identification of known chimeras also allow for the use of DNA-Seq or RNA-Seq sequencing datasets from bulk or single cell datasets. Finally, ChiTaH was also found to be efficient for the identification of sense-antisense (SAS) chimeras, given of its unique reference-based approach (52).

CONCLUSIONS

In this report, we introduced ChiTaH, a fast and accurate method for the discovery of known human chimeras or fusion genes using DNA-Seq or RNA-Seq data generated using NGS technologies. ChiTaH, a user-friendly pipeline that will enable other research groups to make discoveries with ease of installation, is publicly available at GitHub (https://github.com/Rajesh-Detroja/ChiTaH).

DATA AVAILABILITY

Supplementary Data are available at NAR online. Programming codes, data and dependencies are available at GitHub (https://github.com/Rajesh-Detroja/ChiTaH).

SUPPLEMENTARY DATA

Supplementary Data are available at NARGAB Online.

ACKNOWLEDGEMENTS

We thank Dr Sumit Mukherjee, Bar-Ilan University, Israel, for his suggestions on comparative analysis of chimera detection methods.

FUNDING

M.F-M. is supported by the Israel Innovation Authority [Kamin grant 66824, 2019–2021].

Conflict of interest statement. None declared.

REFERENCES

1. Maher,C.A., Kumar-Sinha,C., Cao,X., Kalyana-Sundaram,S., Han,B., Jing,X., Sam,L., Barrette,T., Palanisamy,N. and Chinnaiyan,A.M. (2009) Transcriptome sequencing to detect gene fusions in cancer. *Nature*, **458**, 97–101.
2. Edgren,H., Murumagi,A., Kangaspeska,S., Nicorici,D., Hongisto,V., Kleivi,K., Rye,I.H., Nyberg,S., Wolf,M., Borresen-Dale,A.-L. *et al.* (2011) Identification of fusion genes in breast cancer by paired-end RNA-sequencing. *Genome Biol.*, **12**, R6.
3. Frenkel-Morgenstern,M., Lacroix,V., Ezkurdia,I., Levin,Y., Gabashvili,A., Prilusky,J., Del Pozo,A., Tress,M., Johnson,R., Guigo,R. *et al.* (2012) Chimeras taking shape: potential functions of proteins encoded by chimeric RNA transcripts. *Genome Res.*, **22**, 1231–1242.
4. Finta,C. and Zaphiropoulos,P.G. (2002) Intergenic mRNA molecules resulting from trans-splicing. *J. Biol. Chem.*, **277**, 5882–5890.
5. Li,H., Wang,J., Ma,X. and Sklar,J. (2009) Gene fusions and RNA trans-splicing in normal and neoplastic human cells. *Cell Cycle*, **8**, 218–222.
6. Lim,T.H., Tien,S.L., Lim,P. and Lim,A.S.T. (2005) The incidence and patterns of BCR/ABL rearrangements in chronic myeloid leukaemia (CML) using fluorescence in situ hybridisation (FISH). *Ann. Acad. Med. Singapore*, **34**, 533–538.
7. Tomlins,S.A., Rhodes,D.R., Perner,S., Dhanasekaran,S.M., Mehra,R., Sun,X.W., Varambally,S., Cao,X., Tchinda,J., Kuefer,R. *et al.* (2005) Recurrent fusion of TMPRSS2 and ETS transcription factor genes in prostate cancer. *Science*, **310**, 644–648.
8. Honeyman,J.N., Simon,E.P., Robine,N., Chiaroni-Clarke,R., Darcy,D.G., Lim,I.I.P., Gleason,C.E., Murphy,J.M., Rosenberg,B.R., Teegan,L. *et al.* (2014) Detection of a recurrent DNAJB1-PRKACA chimeric transcript in fibrolamellar hepatocellular carcinoma. *Science*, **343**, 1010–1014.
9. Zhao,Z., Verma,V. and Zhang,M. (2015) Anaplastic lymphoma kinase: role in cancer and therapy perspective. *Cancer Biol. Ther.*, **16**, 1691–1701.
10. Zhong,E. and Huang,H. (2016) Crizotinib in ROS1 rearranged non-small cell lung cancer (NSCLC), from response to resistance. *BMJ Case Rep.*, **2016**, bcr2016217322.
11. Druker,B.J., Guilhot,F., O'Brien,S.G., Gathmann,I., Kantarjian,H., Gattermann,N., Deininger,M.W.N., Silver,R.T., Goldman,J.M., Stone,R.M. *et al.* (2006) Five-Year Follow-up of patients receiving imatinib for chronic myeloid leukemia. *N. Engl. J. Med.*, **355**, 2408–2417.
12. Gross,S., Rahal,R., Stransky,N., Lengauer,C. and Hoeflich,K.P. (2015) Targeting cancer with kinase inhibitors. *J. Clin. Invest.*, **125**, 1780–1789.
13. Rowley,J.D. (1973) A new consistent chromosomal abnormality in chronic myelogenous leukaemia identified by quinacrine fluorescence and giemsa staining. *Nature*, **243**, 290–293.
14. Parker,B.C. and Zhang,W. (2013) Fusion genes in solid tumors: an emerging target for cancer diagnosis and treatment. *Chin. J. Cancer*, **32**, 594–603.
15. Davidson,N.M., Majewski,I.J. and Oshlack,A. (2015) JAFFA: high sensitivity transcriptome-focused fusion gene detection. *Genome Med.*, **7**, 43.
16. Haas,B., Dobin,A., Stransky,N., Li,B., Yang,X., Tickle,T., Bankapur,A., Ganote,C., Doak,T., Pochet,N. *et al.* (2017) STAR-Fusion: fast and accurate fusion transcript detection from RNA-Seq. bioRxiv doi: https://doi.org/10.1101/120295, 24 March 2017, preprint: not peer reviewed.
17. Francis,R.W., Thompson-Wicking,K., Carter,K.W., Anderson,D., Kees,U.R. and Beesley,A.H. (2012) Fusionfinder: a software tool to identify expressed gene fusion candidates from RNA-seq data. *PLoS One*, **7**, 39987.
18. Vu,T.N., Deng,W., Trac,Q.T., Calza,S. and Hwang,W. (2018) A fast detection of fusion genes from paired-end RNA-seq data. *BMC Genomics*, **19**, 786.
19. Benelli,M., Pescucci,C., Marseglia,G., Severgnini,M., Torricelli,F. and Magi,A. (2012) Discovering chimeric transcripts in paired-end RNA-seq data by using ericscript. *Bioinformatics*, **28**, 3232–3239.
20. Nicorici,D., Satalan,M., Edgren,H., Kangaspeska,S., Murumagi,A., Kallioniemi,O., Virtanen,S. and Kilkku,O. (2014) FusionCatcher - a tool for finding somatic fusion genes in paired-end RNA-sequencing data. bioRxiv doi: https://doi.org/10.1101/011650, 19 November 2014, preprint: not peer reviewed.
21. Jia,W., Qiu,K., He,M., Song,P., Zhou,Q., Zhou,F., Yu,Y., Zhu,D., Nickerson,M.L., Wan,S. *et al.* (2013) SOAPfuse: an algorithm for identifying fusion transcripts from paired-end RNA-Seq data. *Genome Biol.*, **14**, R12.
22. Wang,K., Singh,D., Zeng,Z., Coleman,S.J., Huang,Y., Savich,G.L., He,X., Mieczkowski,P., Grimm,S.A., Perou,C.M. *et al.* (2010) MapSplice: accurate mapping of RNA-seq reads for splice junction discovery. *Nucleic Acids Res.*, **38**, e178.
23. Kim,D. and Salzberg,S.L. (2011) TopHat-Fusion: an algorithm for discovery of novel fusion transcripts. *Genome Biol.*, **12**, R72.
24. McPherson,A., Hormozdiari,F., Zayed,A., Giuliany,R., Ha,G., Sun,M.G.F., Griffith,M., Moussavi,A., Senz,J., Melnyk,N. *et al.* (2011) Defuse: an algorithm for gene fusion discovery in tumor rna-seq data. *PLoS Comput. Biol.*, **7**, 1001138.
25. Ge,H., Liu,K., Juan,T., Fang,F., Newman,M. and Hoeck,W. (2011) FusionMap: detecting fusion genes from next-generation sequencing data at base-pair resolution. *Bioinformatics*, **27**, 1922–1928.

26. Sboner,A., Habegger,L., Pflueger,D., Terry,S., Chen,D.Z., Rozowsky,J.S., Tewari,A.K., Kitabayashi,N., Moss,B.J., Chee,M.S. *et al.* (2010) FusionSeq: a modular framework for finding gene fusions by analyzing paired-end RNA-sequencing data. *Genome Biol.*, **11**, R104.
27. Liu,C., Ma,J., Chang,C.C.J. and Zhou,X. (2013) FusionQ: a novel approach for gene fusion detection and quantification from paired-end RNA-Seq. *BMC Bioinformatics*, **14**, 193.
28. Abate,F., Acquaviva,A., Paciello,G., Foti,C., Ficarra,E., Ferrarini,A., Delledonne,M., Iacobucci,I., Soverini,S., Martinelli,G. *et al.* (2012) Bellerophontes: an RNA-Seq data analysis framework for chimeric transcripts discovery based on accurate fusion model. *Bioinformatics*, **28**, 2114–2121.
29. Iyer,M.K., Chinnaiyan,A.M. and Maher,C.A. (2011) ChimeraScan: a tool for identifying chimeric transcription in sequencing data. *Bioinformatics*, **27**, 2903.
30. Piazza,R., Pirola,A., Spinelli,R., Valletta,S., Redaelli,S., Magistroni,V. and Gambacorti-Passerini,C. (2012) FusionAnalyser: a new graphical, event-driven tool for fusion rearrangements discovery. *Nucleic Acids Res.*, **40**, e123.
31. McPherson,A., Wu,C., Wyatt,A.W., Shah,S., Collins,C. and Sahinalp,S.C. (2012) NFuse: discovery of complex genomic rearrangements in cancer using high-throughput sequencing. *Genome Res.*, **22**, 2250–2261.
32. Li,Y., Chien,J., Smith,D.I. and Ma,J. (2011) FusionHunter: identifying fusion transcripts in cancer using paired-end RNA-seq. *Bioinformatics*, **27**, 1708–1710.
33. Wu,J., Zhang,W., Huang,S., He,Z., Cheng,Y., Wang,J., Lam,T.W., Peng,Z. and Yiu,S.M. (2013) SOAPfusion: a robust and effective computational fusion discovery tool for RNA-seq reads. *Bioinformatics*, **29**, 2971–2978.
34. Chen,K., Wallis,J.W., Kandoth,C., Kalicki-veizer,J.M., Mungall,K.L., Mungall,A.J., Jones,S.J., Marra,M.A., Ley,T.J., Mardis,E.R. *et al.* (2012) Breakfusion: targeted assembly-based identification of gene fusions in whole transcriptome paired-end sequencing data. *Bioinformatics*, **28**, 1923–1924.
35. Liu,S., Tsai,W.H., Ding,Y., Chen,R., Fang,Z., Huo,Z., Kim,S., Ma,T., Chang,T.Y., Priedigkeit,N.M. *et al.* (2015) Comprehensive evaluation of fusion transcript detection algorithms and a meta-caller to combine top performing methods in paired-end RNA-seq data. *Nucleic Acids Res.*, **44**, e47.
36. Kumar,S., Vo,A.D., Qin,F. and Li,H. (2016) Comparative assessment of methods for the fusion transcripts detection from RNA-Seq data. *Sci. Rep.*, **6**, 1–10.
37. Haas,B.J., Dobin,A., Li,B., Stransky,N., Pochet,N. and Regev,A. (2019) Accuracy assessment of fusion transcript detection via read-mapping and de novo fusion transcript assembly-based methods. *Genome Biol.*, **20**, 1–16.
38. Mertens,F., Johansson,B., Fioretos,T. and Mitelman,F. (2015) The emerging complexity of gene fusions in cancer. *Nat. Rev. Cancer*. **15**, 371–381.
39. Balamurali,D., Gorohovski,A., Detroja,R., Palande,V., Raviv-Shay,D. and Frenkel-Morgenstern,M. (2020) ChiTaRS 5.0: the comprehensive database of chimeric transcripts matched with druggable fusions and 3D chromatin maps. *Nucleic Acids Res.*, **48**, D825–D834.
40. Kent,W.J. (2002) BLAT—the BLAST-Like alignment tool. *Genome Res.*, **12**, 656–664.
41. Altschul,S.F., Gish,W., Miller,W., Myers,E.W. and Lipman,D.J. (1990) Basic local alignment search tool. *J. Mol. Biol.*, **215**, 403–410.
42. Langmead,B. and Salzberg,S.L. (2012) Fast gapped-read alignment with bowtie 2. *Nat. Methods*, **9**, 357–359.
43. Quinlan,A.R. and Hall,I.M. (2010) BEDTools: a flexible suite of utilities for comparing genomic features. *Bioinformatics*, **26**, 841–842.
44. Li,H. and Durbin,R. (2009) Fast and accurate short read alignment with burrows-wheeler transform. *Bioinformatics*, **25**, 1754–1760.
45. Dobin,A., Davis,C.A., Schlesinger,F., Drenkow,J., Zaleski,C., Jha,S., Batut,P., Chaisson,M. and Gingeras,T.R. (2013) STAR: ultrafast universal RNA-seq aligner. *Bioinformatics*, **29**, 15–21.
46. Madeira,F., Park,Y.M., Lee,J., Buso,N., Gur,T., Madhusoodanan,N., Basutkar,P., Tivey,A.R.N., Potter,S.C., Finn,R.D. *et al.* (2019) The EMBL-EBI search and sequence analysis tools APIs in 2019. *Nucleic Acids Res.*, **47**, W636–W641.
47. Lever,J., Zhao,E.Y., Grewal,J., Jones,M.R. and Jones,S.J.M. (2019) CancerMine: a literature-mined resource for drivers, oncogenes and tumor suppressors in cancer. *Nat. Methods*, **16**, 505–507.
48. Liao,Y., Wang,J., Jaehnig,E.J., Shi,Z. and Zhang,B. (2019) WebGestalt 2019: gene set analysis toolkit with revamped UIs and APIs. *Nucleic Acids Res.*, **47**, W199–W205.
49. Frenkel-Morgenstern,M., Gorohovski,A., Lacroix,V., Rogers,M., Ibanez,K., Boullosa,C., Leon,E.A., Ben-Hur,A. and Valencia,A. (2013) ChiTaRS: a database of human, mouse and fruit fly chimeric transcripts and RNA-sequencing data. *Nucleic Acids Res.*, **41**, 142–151.
50. Frenkel-Morgenstern,M., Gorohovski,A., Vucenovic,D., Maestre,L. and Valencia,A. (2015) ChiTaRS 2.1-an improved database of the chimeric transcripts and RNA-seq data with novel sense-antisense chimeric RNA transcripts. *Nucleic Acids Res.*, **43**, D68–D75.
51. Gorohovski,A., Tagore,S., Palande,V., Malka,A., Raviv-Shay,D. and Frenkel-Morgenstern,M. (2017) ChiTaRS-3.1-the enhanced chimeric transcripts and RNA-seq database matched with protein-protein interactions. *Nucleic Acids Res.*, **45**, D790–D795.
52. Mukherjee,S., Detroja,R., Balamurali,D., Matveishina,E., Medvedeva,Y.A., Valencia,A., Gorohovski,A. and Frenkel-Morgenstern,M. (2021) Computational analysis of sense-antisense chimeric transcripts reveals their potential regulatory features and the landscape of expression in human cells. *NAR Genomics Bioinforma.*, **3**, lqab074.